Biochem. J. (1984) **224**, 877–886
Printed in Great Britain

The mechanism of *Klebsiella pneumoniae* nitrogenase action

Pre-steady-state kinetics of H_2 formation

David J. LOWE and Roger N. F. THORNELEY
A.F.R.C. Unit of Nitrogen Fixation, University of Sussex, Brighton BN1 9RQ, U.K.

(*Received 6 June 1984/Accepted 24 August 1984*)

A comprehensive model for the mechanism of nitrogenase action is used to simulate pre-steady-state kinetic data for H_2 evolution in the presence and in the absence of N_2, obtained by using a rapid-quench technique with nitrogenase from *Klebsiella pneumoniae*. These simulations use independently determined rate constants that define the model in terms of the following partial reactions: component protein association and dissociation, electron transfer from Fe protein to MoFe protein coupled to the hydrolysis of MgATP, reduction of oxidized Fe protein by $Na_2S_2O_4$, reversible N_2 binding by H_2 displacement and H_2 evolution. Two rate-limiting dissociations of oxidized Fe protein from reduced MoFe protein precede H_2 evolution, which occurs from the free MoFe protein. Thus Fe protein suppresses H_2 evolution by binding to the MoFe protein. This is a necessary condition for efficient N_2 binding to reduced MoFe protein.

We present in this and the following papers (Thorneley & Lowe, 1984*a*,*b*; Lowe & Thorneley, 1984) kinetic data obtained with nitrogenase for H_2 evolution and N_2 reduction. These data have been used to formulate a mechanism for nitrogenase action. At the outset it should be stressed that this mechanism does not define the detailed sequence of chemical events occurring at the substrate reduction site during the catalytic cycle. We have calculated the time courses for the oxidation and reduction of both the Fe protein (Kp2, M_r 68000, 4Fe atoms/molecule) and the MoFe protein (Kp1, M_r 218000, 32Fe and 2Mo atoms/molecule) by using independently determined rate constants and assigned to various intermediate forms of Kp1 the ability to evolve H_2 and bind and reduce N_2. This makes it possible to simulate the observed time courses for the production of H_2 and NH_3 obtained with the rapid-quench technique. In addition, the unusual damped oscillation exhibited by the concentration of an enzyme-bound intermediate that is formed during N_2 reduction, and that yields N_2H_4 on quenching in acid or alkali, has been simulated (Thorneley *et al.*, 1978; Thorneley & Lowe, 1984*a*). The mechanism explains why the steady-state rates of H_2 evolution and N_2 reduction depend on the concentration of the electron donor ($Na_2S_2O_4$) and the concentration and ratio of the component proteins Kp1 and Kp2. An explanation for the extremely long turnover time (approx. 1.5s to reduce N_2 to $2NH_3$) and the high concentration of nitrogenase *in vivo* (approx. 100 μM) is also suggested.

An important aspect of nitrogenase action is the relationship between H_2 evolution and N_2 reduction. In the absence of N_2, nitrogenase catalyses the reduction of protons to H_2 (eqn. 1):

$$2H^+ + 2e^- \rightarrow H_2 \qquad (1)$$

In the presence of N_2, H_2 evolution is partially suppressed, such that the limiting stoichiometry given by eqn. (2) is observed (Rivera-Ortiz & Burris, 1975; Burgess *et al.*, 1981; Guth & Burris, 1983):

$$8H^+ + N_2 + 8e^- \rightarrow 2NH_3 + H_2 \qquad (2)$$

Eqns. (1) and (2) represent nitrogenase-catalysed reductions that are MgATP-dependent. Under optimal conditions, for every 2 electron equivalents transferred to reducible substrates, 4 equivalents of MgATP are hydrolysed to $MgADP + P_i$ (Watt *et al.*, 1975).

Abbreviations used: the nitrogenase components of the various organisms are denoted by a capital letter indicating the genus and a lower-case letter indicating the species, and the number 1 indicates the MoFe-containing protein and the number 2 the Fe-containing protein: Kp, *Klebsiella pneumoniae*; Av, *Azotobacter vinelandii*; Cp, *Clostridium pasteurianum*.

A feature of the reduction of the alternative substrates, acetylene (Hageman & Burris, 1980) and azide (Dilworth & Thorneley, 1981), is that, although the percentage of electrons directed into a particular substrate varies with the relative concentrations of substrates, the total electron flux through nitrogenase remains unaltered. The electron flux is determined by the ratio of the component proteins and the nature and concentration of the electron donor. This suggests a common, substrate-independent, rate-limiting step. This has recently been identified as the dissociation of oxidized Fe protein with MgADP bound from the reduced MoFe protein (Thorneley & Lowe, 1983). This step is the third partial reaction in Scheme 1, which shows a cycle in which one electron is transferred from Kp2 to Kp1† with the concomitant hydrolysis of 2MgATP to 2MgADP + 2P_i (Eady *et al.*, 1978*a*; Hageman *et al.*, 1980).

Scheme 1, which we call the Fe-protein cycle (Thorneley & Lowe, 1983) forms the basic unit of the MoFe-protein cycle. In order to effect the reaction shown in eqn. (2), eight electrons are required. This is achieved by eight sequential cycles of Scheme 1, which, when coupled together, comprise one MoFe-protein cycle in which one N_2 molecule is reduced (Scheme 2).

In the present paper we present pre-steady-state kinetic data for H_2 evolution in the absence and in the presence of N_2 and simulate these data by using Scheme 2. A detailed description of Scheme 2 is restricted to those aspects that are concerned with H_2 evolution.

Methods and materials

Protein preparation

The nitrogenase component proteins were purified as described by Eady *et al.* (1972), with an additional DEAE-cellulose chromatography step (Smith *et al.*, 1976). Gel filtration (Sephadex G-25) was used to prepare stock solutions of Kp1 protein (45mg/ml) and Kp2 protein (27mg/ml) in 25mM-Hepes [4-(2-hydroxyethyl)-1-piperazine-ethanesulphonic acid]/NaOH buffer, pH7.4, containing 10mM-$MgCl_2$ and 1mM-$Na_2S_2O_4$. Kp1 and Kp2 proteins had specific activities of 1700 and 1500nmol of C_2H_2 reduced/min per mg of protein respectively when assayed at 30°C under the standard conditions given by Eady *et al.* (1972). Protein stock solution (0.01ml) was assayed before and after each rapid-quench experiment by a standard C_2H_2-reduction assay (Eady *et al.*, 1972) of 2min duration at 30°C. The molybdenum content of the Kp1 protein was determined to be 1.4 ± 0.1 g-atom of Mo/mol of protein by using the method of Clarke & Axley (1955).

All biochemicals were purchased from Sigma Chemical Co., Kingston-upon-Thames, Surrey, U.K., and salts from BDH Chemicals, Poole, Dorset, U.K.

Rapid-quench technique

The apparatus represented schematically in Fig. 1 is essentially that described by Gutteridge *et al.* (1978) for the rapid-freezing of protein samples in isopentane at −140°C before the running of e.p.r. spectra. The 'stepping motor' is controlled electronically and delivers a pre-set volume of solution from each syringe at a defined velocity through a mixing chamber and down a length of thick-walled nylon capillary tubing of variable length. The solution emerges from a stainless-steel needle jet into a small volume of quenching agent contained in a glass vial fitted with a gas-tight rubber closure. Typically, mixed protein/substrate solution (0.4ml) was shot into 1M-$HClO_4$ quenching agent (0.5ml). This procedure quenches nitrogenase activity within 2ms (Eady *et al.*, 1978*a*). Each shot

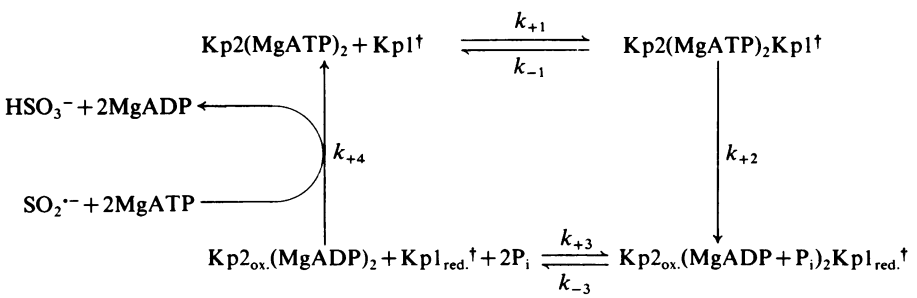

Scheme 1. *Oxidation–reduction cycle for the Fe protein*

Kp1† represents one of two independently functioning halves of the tetrameric ($\alpha_2\beta_2$ structure) Kp1. Each Kp1† is assumed to contain one Mo substrate-binding site and one Kp2-binding site. Table 1 contains the values of all the rate constants in Scheme 1.

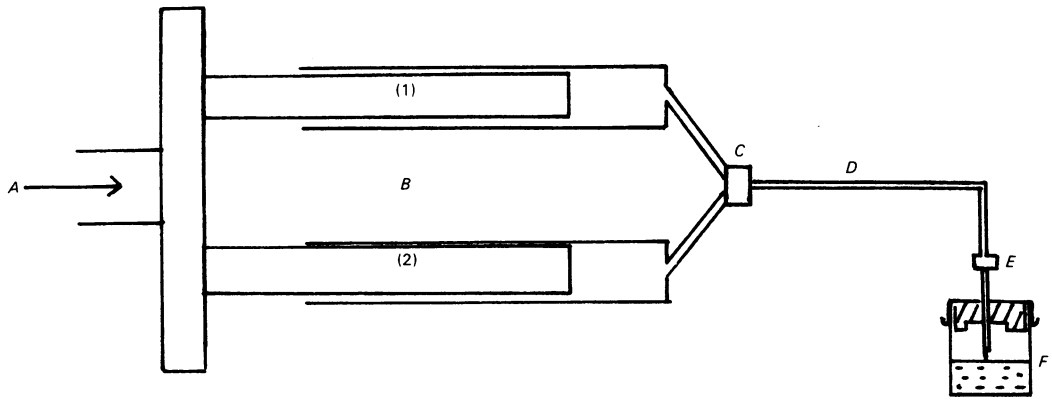

Fig. 1. *Schematic representation of the rapid-quench apparatus for pre-steady-state kinetic studies*
Key: *A*, electronically controlled ram driven by a stepping motor; *B*, thermostatically maintained drive syringes containing (1) Kp1 and Kp2 proteins, $Na_2S_2O_4$, $MgCl_2$ and Hepes buffer, pH 7.4, and (2) ATP, $Na_2S_2O_4$, $MgCl_2$ and Hepes buffer, pH 7.4; *C*, mixing chamber; *D*, reaction tube of variable length made from thick-wall capillary nylon tube; *E*, jet made from 22-gauge stainless-steel needle; *F*, quenching agent contained in glass vial fitted with gas-tight rubber closure.

produced a single datum point on a reaction progress curve.

After quenching, equilibration of H_2 between the liquid and gas phase was achieved by vigorous shaking of the inverted vials for 15 min. The use of small-volume (2.3 ml) vials increased the sensitivity of detection, since a larger proportion of the total product was injected into the vapour-phase chromatography apparatus. The increased pressure of the gas phase resulting from the injection of the mixed protein/substrate solution (0.4 ml) was compensated for by taking the same volume of gas out for analysis. A Pye–Unicam PU4500 chromatograph with a 5A molecular-sieve (60–80 mesh) column was used for H_2 analysis. Each rapid quench shot generally contained approx. 10 nmol of MoFe protein and 40 nmol of Fe protein, and the reduction product, H_2, was analysed to an accuracy of ± 1 nmol per shot. Quantitative recovery and accurate determination of H_2 was demonstrated by control experiments from which ATP was omitted: standard volumes of water, saturated with H_2 at 20°C, were added to the liquid phase in the vials after quenching, and, after equilibration by shaking, the H_2 in the gas was determined as described above. The solutions in the drive syringes were saturated with N_2, H_2 or Ar by evacuation and flushing on an all-glass vacuum line.

Computing

The linear differential equations describing Schemes 1 and 2 and those for the dissociation of $S_2O_4^{2-}$ to give the active reductant $SO_2^{\cdot-}$ (Thorneley & Lowe, 1983) were solved by using NAG subroutines DO2ABF and DO2BAF on PDP 1134A and VAX 780 computers. In all the simulations in this and the following papers (Thorneley & Lowe, 1984*a*,*b*; Lowe & Thorneley, 1984) the curves have been adjusted by allowing the concentrations of $Kp1^{\dagger}$ and Kp2 to vary by $\pm 10\%$ from the measured values. This enables a fair comparison of data with computed simulations after considering the experimental errors. The $Kp1^{\dagger}$ concentration was taken to be the Mo concentration, i.e. Kp1 was 70% active. The Kp2 was 45% active on the basis of a maximum specific activity of 3500 nmol of H_2/min per mg of Kp2. Inactive Kp1 was assumed not to bind to Kp2. Inactive Kp2 was assumed to bind to $Kp1^{\dagger}$ with the same association and dissociation rate constants as active $Kp2_{ox.}$. These assumptions were necessary in order to simulate the inhibition of substrate reduction observed at high protein concentrations (Lowe & Thorneley, 1984).

A feature of the simulations is a damped oscillatory approach to the steady state. This is caused by the sequential nature of the mechanism involving multiple intermediate states of the enzyme that become significantly populated in the steady state. At time zero, the enzyme is present in a single state. After initiation of the reaction, the intermediate states become populated in a damped oscillatory manner. The familiar burst and lag phases (Cornish-Bowden, 1979) observed in other enzyme systems are examples of this effect with a high degree of damping because of the smaller number of intermediates and the values of the rate constants involved.

Results and discussion

Pre-steady-state kinetics

Fig. 2 shows data points for the time course for H_2 formation under an Ar atmosphere when the proton is the only reducible substrate. A lag of 100ms is followed by a linear phase, which represents a constant rate of H_2 formation of 460nmol of H_2/min per mg of Kp1. This rate was maintained for at least 10s, demonstrating that no significant product inhibition by MgADP or exhaustion of $S_2O_4^{2-}$ had occurred during this time. This is important, since this rate of H_2 production is significantly lower than that predicted from the specific activities of the protein samples taken from a drive syringe at the end of a series of rapid-quench shots and assayed as described in the Methods and materials section. The difference is due to the dependence of the activity of Kp1 on the absolute concentrations as well as the ratio of Fe protein to MoFe protein (Thorneley & Lowe, 1984*b*). At protein concentrations above 10μM the rate of complex-formation between $Kp2_{ox.}(MgADP)_2$ and $Kp1^{\dagger}$ (k_{+3} in Scheme 1) can become significant compared with the rate-limiting complex dissociation reaction (k_{-3}) and the rate of reduction of $Kp2_{ox.}(MgADP)_2$ by $SO_2^{\cdot-}$ (k_{-4}). This decreases the rate of substrate reduction under the conditions of high protein concentration used in the rapid-quench experiments. The activity control assays used protein concentrations 50–100 times lower than those used for rapid-quench experiments, and with these low protein concentrations no inhibition of substrate reduction occurs.

Fig. 3 shows the time course for H_2 formation under an atmosphere of N_2, when NH_3 is also a reduction product. The early part of the time course is the same as that shown in Fig. 2 (lag of 100ms); however, the steady-state rate of 460nmol of H_2/min per mg of Kp1 is maintained for only 400ms, after which it decreases until at 1500ms the rate is 270nmol of H_2/min per mg of Kp1, which is then maintained up to at least 10s.

The lines in Figs. 2 and 3 have not been fitted to the data points, but are computer simulations based on Schemes 1 and 2 together with the independently determined rate constants in Table 1.

MoFe-protein cycle

Scheme 2 shows the MoFe-protein cycle. The complete scheme is presented here so that the reader can appreciate how the results of H_2 evolution fit into the overall scheme required for N_2 reduction. In the present paper we describe only those parts of Scheme 2 that are relevant to H_2 evolution. The reader is referred to the following

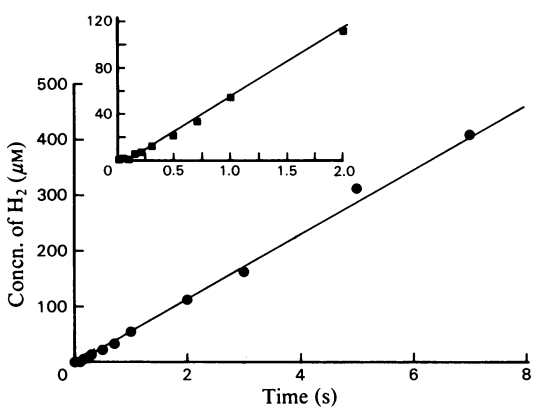

Fig. 2. *Pre-steady-state time course for H_2 evolution under Ar at 23°C at pH7.4*

The inset shows a pre-steady-state lag phase of 100ms followed by a steady-state rate of H_2 evolution of 460nmol/min per mg of Kp1. The data were obtained with the rapid-quench technique as described in the Methods and materials section. The line through the data points is a computed simulation made by using Scheme 2 and the rate constants in Table 1. Before mixing syringe *A* contained 68μM-Kp1, 266μM-Kp2, 1mM-$Na_2S_2O_4$, 10mM-$MgCl_2$ and 25mM-Hepes buffer, pH7.4. Syringe *B* contained 18mM-ATP, 19mM-$Na_2S_2O_4$, 10mM-$MgCl_2$ and 25mM-Hepes buffer, pH7.4.

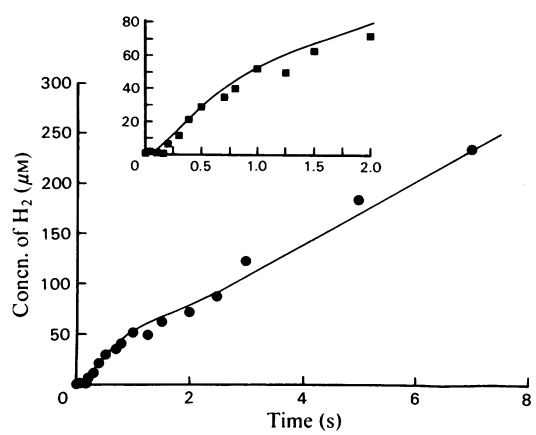

Fig. 3. *Pre-steady-state time course for H_2 evolution under N_2 at 23°C at pH7.4*

The inset shows a pre-steady-state lag phase of 100ms, then a burst phase that is essentially complete at 2.0s, followed by a steady-state rate of H_2 evolution of 270nmol/min per mg of Kp1. The line through the data points is a computed simulation made by using Scheme 2 and the rate constants in Table 1. Concentrations of reactants were as described for Fig. 2.

Table 1. *Rate constants used in the simulation of the kinetics of Kp nitrogenase at 23°C at pH7.4*

The differences between the values of some of the rate constants shown and those reported previously (Lowe *et al.*, 1984) are due to the more accurate determination of k_{+1}.

Rate constant	Value	Comment	Reference
k_{+1}	$5\times10^{7}\,M^{-1}\cdot s^{-1}$*	Responsible for dilution effect	Lowe & Thorneley (1984)
k_{-1}	$15\,s^{-1}$*		
k_{+2}	$200\,s^{-1}$	Electron transfer coupled to MgATP hydrolysis	Thorneley (1975)
k_{+3}	$4.4\times10^{6}\,M^{-1}\cdot s^{-1}$*	Responsible for inhibition at high protein concentrations	Thorneley & Lowe (1983)
k_{-3}	$6.4\,s^{-1}$*	Rate-limiting when Kp2 and substrates are saturating	
k_{+4}	$3.0\times10^{6}\,M^{-1}\cdot s^{-1}$	Rate of reduction of $Kp2_{ox.}$ $(MgADP)_2$ by $SO_2^{\cdot-}$	
k_{+5}	$4.4\times10^{6}\,M^{-1}\cdot s^{-1}$	Responsible for inhibition of H_2 evolution when MgATP but not reductants is limiting	
k_{-5}	$6.4\,s^{-1}$*		
k_{+6}	$1.2\times10^{9}\,M^{-1}\cdot s^{-1}$	$S_2O_4^{2-} \underset{k_{+6}}{\overset{k_{-6}}{\rightleftharpoons}} 2SO_2^{\cdot-}$	
k_{-6}	$1.7\,s^{-1}$		
k_{+7}	$250\,s^{-1}$†	Responsible for enhanced H_2 evolution at low e^- flux	Thorneley & Lowe (1984*a*) Lowe & Thorneley (1984)
k_{+8}	$8.0\,s^{-1}$†	Slow in order to maximize N_2 binding to E_3	
k_{+9}	$400\,s^{-1}$†‡	Rapid H_2 evolution from the most-reduced hydridic species	
k_{+10}	$4\times10^{5}\,M^{-1}\cdot s^{-1}$	Determined from $K_m^{N_2}$ at low e^- flux	
k_{-10}	$8\times10^{4}\,M^{-1}\cdot s^{-1}$	Determined from $K_i^{H_2}$ at low e^- flux	
k_{+11}	$2.2\times10^{6}\,M^{-1}\cdot s^{-1}$‡	Determined from $K_m^{N_2}$ at high e^- flux	
k_{-11}	$3.0\times10^{6}\,M^{-1}\cdot s^{-1}$‡	Determined from $K_i^{H_2}$ at high e^- flux	

* Kp1–Kp2 association–dissociation rates assumed to be independent of Kp1 oxidation level.

† H_2-evolution rates. These depend on small differences between large numbers and are subject to errors of factors of about 2.

‡ Since these rate constants determine K_m and K_i values only their ratios are absolute values.

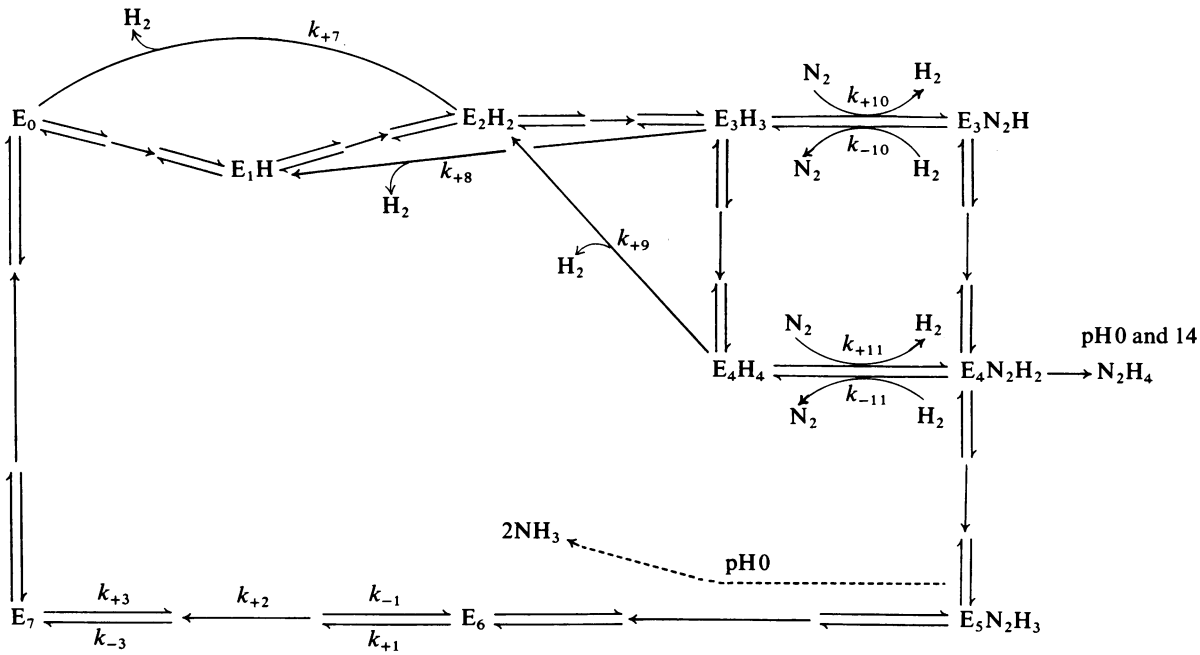

Scheme 2. *MoFe-protein cycle for nitrogenase*

papers (Thorneley & Lowe, 1984*a*,*b*; Lowe & Thorneley, 1984) for complete descriptions of other aspects of Scheme 2 and for details of the determination of some of the rate constants in Table 1. The third paper in this series (Lowe & Thorneley, 1984) includes a critique of Scheme 2, and presents a mechanism for nitrogenase-catalysed $^1H^2H$ formation from $^2H_2$.

The species E_n in Scheme 2 represents one of two independently functioning halves ($Kp1^{\dagger}$) of the tetrameric ($\alpha_2\beta_2$ structure) Kp1 and therefore contains one substrate-binding site. This assumption is required in order to simulate the steady-state concentration of an intermediate in N_2 reduction that yields N_2H_4 on quenching and is discussed in the following paper (Thorneley & Lowe, 1984*a*). The related assumption that Kp2 can bind at two independent sites on Kp1 (Scheme 1) has been discussed previously (Thorneley & Lowe, 1983). The subscript *n* refers to the number of times $Kp1^{\dagger}$ protein has completed the electron-transfer cycle shown in Scheme 1. Therefore the subscript refers to the number of slow rate-limiting protein dissociation steps (k_{-3}) that $Kp1^{\dagger}$ has undergone. The subscript also indicates the number of electron equivalents by which $Kp1^{\dagger}$ has been reduced relative to the resting E_0, which is that of Kp1 as isolated in the presence of $S_2O_4^{2-}$. The use of eight slow steps such that *n* has values from 0 to 7 is required for two reasons. Firstly, eight electrons are necessary for reduction of N_2 and stoichiometric evolution of H_2 (eqn. 2). Secondly, significantly better simulations for the time course for N_2H_4 formation (produced on quenching an enzyme-bound intermediate in N_2 reduction; Thorneley *et al.*, 1978) were obtained with Scheme 2 than with a scheme comprising six slow steps (Thorneley & Lowe, 1984*a*).

The three reactions represented by the arrows linking E_n with E_{n+1} ($n = 0$ to 7, with $E_8 = E_0$) in Scheme 2 are reactions 1, 2 and 3 respectively of Scheme 1. The values of k_{+1}, k_{-1}, k_{+2}, k_{+3} and k_{-3} (Table 1) are assumed to be independent of the level of reduction of Kp1.

The designation of species E_n as E_nH_n ($n = 1, 2, 3$ or 4) does not necessarily imply that Scheme 2 requires metal hydride intermediates. The simulations of the time courses for H_2 evolution (Figs. 2 and 3) only require that species E_1 does not evolve H_2 and that species E_2, E_3 and E_4 can all evolve H_2 at different rates (k_{+7}, k_{+8} and k_{+9}; Table 1), by reactions in which $Kp1^{\dagger}$ is oxidized by 2 electron equivalents. The possible nature of the bound hydrogen on species E_2H_n ($n = 1$, 2, 3 or 4) is discussed in the following papers (Thorneley & Lowe, 1984*a*,*b*; Lowe & Thorneley, 1984).

Scheme 2 requires that a distinction must be made between H_2 evolved at pH7.4 and H_2 released on quenching with acid. This is shown in Fig. 4, in which computer simulations of H_2 time courses are shown. Curve (*a*) is identical with that shown with the experimental data points in Fig. 2,

and is the total H_2 obtained when enzyme turning over at pH7.4, in the absence of N_2, is quenched with acid. Curve (*a*) is summation of curves (*b*) and (*c*). Curve (*c*) is the H_2 that is evolved at pH7.4 before the quenching. It is the curve that would be obtained from a rapidly responding H_2 electrode monitoring the enzyme at pH7.4 (the development of such an electrode would be extremely useful for further verification of Scheme 2). Curve (*b*) is the additional H_2 that is liberated on quenching with acid. Species E_2H_2 and E_3H_3 are each assumed to evolve 1, and species E_4H_4 2, equivalents of H_2 on quenching.

Species E_1H cannot evolve H_2 either at pH7.4 during turnover or on quenching, since, if this were the case, no lag phase in Figs. 2 and 3 would be observed. Two sequential slow steps with rate constants close to $6.4s^{-1}$ are required to simulate the lag phases in Figs. 2 and 3. We have considered the possibility that, since we premixed Kp1 with Kp2 in one syringe of the rapid-quench apparatus, the complex between these proteins has first to dissociate before MgATP can bind and that E_1H would then be formed after two slow dissociations under our experimental conditions. However, this is not possible, since in stopped-flow spectrophotometric experiments Thorneley (1975) showed that premixed Kp1 and Kp2, when shot against MgATP, exhibited rapid electron transfer from Kp2 to Kp1 ($k_2 = 2 \times 10^2 s^{-1}$), with no evidence for a slow predissociation of the two proteins.

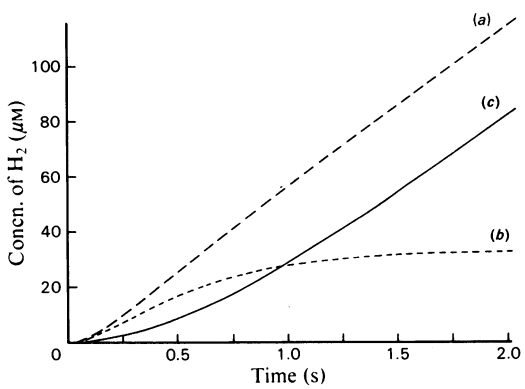

Fig. 4. *Distinction between between H_2 evolved at pH7.4 and that liberated from intermediates by acid quench*
Computer simulations made by using Scheme 2 and the rate constants in Table 1 are shown. Curve (*a*), total H_2 determined in rapid-quench experiments under Ar; the curve is a summation of curves (*b*) and (*c*) and identical with that in Fig. 2. Curve (*b*), H_2 liberated from species E_2H_2, E_3H_3 and $E_4H_3^-$ by reaction with acid quench. Curve (*c*), H_2 evolved at pH7.4 by functioning nitrogenase. Simulations are for the protein concentrations and conditions described in the legend to Fig. 2.

Hageman & Burris (1978), using an [Av1]/[Av2] ratio of 100:1, obtained a lag phase of H_2 evolution of 4min. Their lag phase should not be confused with the lag phases in Figs. 2 and 3, in which a [Kp2]/[Kp1] ratio of 4:1 was used. Under the conditions employed by Hageman & Burris (1978), Scheme 2 shows that the second-order reaction (k_{+1}) between reduced $Av2(MgATP)_2$ and Av1 (at state E_1H) is rate-limiting. A steady state is only attained after several minutes when the concentration of E_0 equals that of E_1H. Hageman & Burris (1978) concluded that the transfer of one electron from the Fe protein to the MoFe protein does not cause H_2 evolution, and that at least one slow dissociation of Av2 from Av1 precedes H_2 evolution. In terms of our model, Hageman & Burris (1978) correctly concluded that H_2 evolution occurs at or after point *A* in Scheme 3. The data in Figs. 2 and 3 allow the further conclusion that two dissociations of the Fe protein from the MoFe protein are necessary before H_2 is evolved, even on quenching with acid. In Scheme 3, this means at or after point *C*. This is because, under our conditions with an excess of Kp2 over Kp1, the two slow steps necessary to generate the 100ms lag phase in H_2 evolution have to be protein dissociation reactions. E_2H_2 is the first species in Scheme 2 that satisfies this criterion. The species at point *B* in Scheme 3 is the complex $Kp2_{ox}.(MgADP)_2$–E_1^-H. This complex cannot evolve H_2 (even on quenching with acid, since it is formed after only one slow protein dissociation step (between E_0 and E_1H), and H_2 evolution at this point would not give a lag phase. Thus, although the MoFe protein in this complex has received two electrons from two successful encounters with Fe protein, it cannot evolve H_2. We propose that it is the presence of oxidized Fe

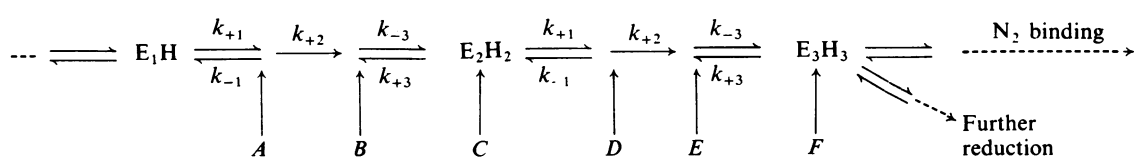

Scheme 3. *Two protein dissociations are required before H_2 is evolved*

protein bound to species $E_1{}^-H$ that prevents H_2 evolution. This is an important role for the Fe protein in addition to that of a specific reductase of the MoFe protein. It has not escaped our attention that the complex at point *B* formed by reaction k_{+3} may have a different structure, and reactivity on quenching, from that formed by reaction k_{+2}. The concentration of the complex formed by k_{+3} is less than 2% of the total $Kp1^{\dagger}$ concentration in the steady state under our conditions. The precision of the data in Figs. 2 and 3 does not allow us to tell whether this complex yields H_2 on quenching. Similarly, the complexes involving inactive Kp2 and E_2H_2 may not yield H_2 on quenching.

H_2 evolution at points *D* and *E* (Scheme 3) would also be consistent with the 100ms lag phase for H_2 evolution, since both these complexes are formed rapidly after only two slow protein dissociation steps (between E_0 and E_1H and between E_1H and E_2H_2). However, since we have had to propose that oxidized Fe protein bound to $E_1{}^-H$ (point *B*, Scheme 3) prevents H_2 evolution, we have also assumed in Scheme 2 that reduced Fe protein bound to E_2H_2 (point *D*, Scheme 3) and oxidized Fe protein bound to $E_2{}^-H_2$ (point *E*, Scheme 3) also prevent H_2 evolution. Thus, throughout Scheme 2, only free $Kp1^{\dagger}$ at all levels of reduction can bind substrates or inhibitors and release products. This now provides an explanation for the important observations made by Silverstein & Bulen (1970) and Hageman & Burris (1980) that, as the electron flux through nitrogenase is decreased by decreasing the Fe protein/MoFe protein ratio, a greater percentage of this flux is directed into H_2 evolution and less into N_2 reduction. This effect is so significant that, under the conditions employed by Hageman & Burris (1978), to generate long lag phases ([Av2]/[Av1] ratio 1:100) very little N_2 is reduced and essentially all the electrons are used for H_2 production. This is a consequence of the competition between the first-order H_2 evolution reaction from species E_2H_2 (k_{+7}) and the second-order reaction of E_2H_2 with reduced Fe protein (k_{+1}), i.e. conversion of *C* into *D* in Scheme 3. The latter reaction forms the complex $Kp2(MgATP)_2$–E_2H_2 (*D*), which cannot evolve H_2. At low [Fe protein]/[MoFe protein] ratios the H_2-evolution reaction (k_{+7}) dominates and the amount of MoFe protein that is further reduced to the N_2-binding states, E_3 and E_4 (Thorneley & Lowe, 1984*a*), is relatively small.

This effect is illustrated in Fig. 5, which shows simulations of the H_2 evolved at pH7.4 as a function of the concentration of Kp1 and Kp2 proteins. These curves are similar to curve (*c*) in Fig. 4 in that the H_2 evolved on quenching is not considered. As the concentration of nitrogenase component proteins is decreased, the lag for H_2 evolution decreases, since the dominant H_2-evolving species becomes E_2H_2, the first H_2-evolving species in Scheme 2. At high protein concentrations the dominant H_2-evolving species are E_3H_3 and E_4H_4. These species are formed after E_2H_2 in Scheme 2 and therefore after a longer lag phase. Since E_3H_3 and E_4H_4 are the N_2-binding species, high protein concentrations favour N_2 reduction relative to H_2 evolution.

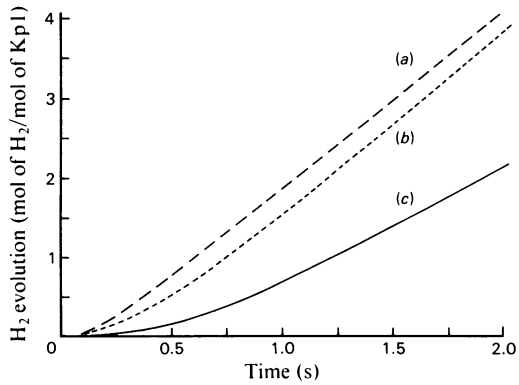

Fig. 5. *H_2 evolution at pH7.4 as a function of nitrogenase concentration*

Computer simulations of pre-steady-state time courses for H_2 evolution made by using Scheme 2 and the rate constants in Table 1 are shown. Curve (*a*), 1.0 μM-Kp1 and 4.0 μM-Kp2; curve (*b*) 10.0 μM-Kp1 and 40.0 μM-Kp2; curve (*c*) 100.0 μM-Kp1 and 400.0 μM-Kp2. As the protein concentration increases, a longer lag phase occurs, since a higher proportion of the H_2 is evolved from the N_2-binding species E_3H_3 and E_4H_4. Curve (*c*) shows a lower final activity than curve (*a*) or (*b*) because of the inhibition at high protein concentrations. These curves are similar to curve (*c*) in Fig. 4. They represent the H_2 evolved by nitrogenase functioning at pH7.4 and do not simulate the total H_2 determined in a rapid-quench experiment.

The second role that we have assigned to the Fe protein, that of preventing H_2 evolution from reduced MoFe protein, is so important that we consider the nomenclature of Hageman & Burris (1978) that describes the Fe protein as 'dinitrogenase reductase' inappropriate and misleading. The role of the Fe protein is, not to act merely as a specific reductase for MoFe protein, but also to cause the MoFe protein to function as nitrogenase not as hydrogenase. We consider that the chemistry occurring at the active site involves metal–hydrogen complexes that are thermodynamically unstable and react with protons to yield H_2 [see the following papers (Thorneley & Lowe, 1984*a*,*b*; Lowe & Thorneley, 1984)]. Protons cannot be excluded from the site, since they are needed to

protonate N_2 and its intermediates to form NH_3, and may also be required to generate the metal dihydride that we propose as a precursor to the binding of N_2 by H_2 displacement. We suggest that the enzyme has evolved to control H_2 production kinetically, and that this can only be achieved if nitrogenase is an extremely slow enzyme present at high concentrations in the cell.

Location of the substrate-reduction and electron-transfer sites

The ability of the Fe protein to suppress H_2 evolution from the complex with MoFe protein suggests that the sites on the MoFe protein that evolve H_2, bind N_2 and accept electrons from the Fe protein are all on or close to that part of the surface of the MoFe protein that interacts with the Fe protein. The report by Miller *et al.* (1980) that tetrameric Kp1 contains four MgATP-binding sites suggests that two of these on each dimeric unit may be complementary to the two MgATP-binding sites on the Fe protein. Therefore the two MgATP molecules may bridge the Fe protein and the MoFe protein, with the electron-transfer and substrate-reduction sites insulated from the solvent within this complex. Since the chemistry of N_2 reduction probably involves low potentials, possibly generated transiently by coupling electron transfer to ATP hydrolysis, it makes good sense to restrict access of solvent and protons to these sites in order to prevent H_2 evolution. The obligate dissociation of oxidized Fe protein from MoFe protein before reduction by $SO_2^{\cdot-}$ can occur (Thorneley & Lowe, 1983) suggests that there is only one electron-transfer site on the Fe protein, i.e. the same site is used to receive an electron from the donor and to transfer an electron to the MoFe protein.

H_2 evolution concomitant with N_2 reduction

The discussion of the data presented in Fig. 3 provides a convenient bridge to the following paper (Thorneley & Lowe, 1984*a*) concerned with N_2 reduction. The stoichiometry indicated by eqn. (2) is approached as the [Fe protein]/[MoFe protein] ratio tends to infinity with saturating N_2. The reason for this is that it is only under these conditions that H_2 evolution from E_2H_2 (k_{+7}), E_3H_3 (k_{+8}) and E_4H_4 (k_{+9}) is effectively suppressed, such that H_2 is only evolved by the N_2-binding reactions k_{+10} and k_{+11}. Under the conditions employed to obtain the data in Fig. 3, this did not occur, and only 42% of the total electron flux went to N_2 reduction and the remaining 58% was used to evolve H_2 after the steady state that has been achieved (approx. 1.5s). Under these conditions H_2 evolution contains contributions from k_{+7}, k_{+8} and k_{+9}. A comparison of Fig. 2 with Fig. 3 shows that the lag phase of 100ms and the initial time course for H_2 evolution (up to 500ms) are essentially the same. Over this period the major sources of H_2 are reaction k_{+7} and the quenching of species E_2H_2 together with its complexes with oxidized and reduced Kp2. At times longer than 1 s the rate of H_2 evolution falls in the presence of N_2 (Fig. 3) as more $Kp1^{\dagger}$ becomes distributed among the species E_n ($n = 3$–7) with N_2, or intermediates in N_2 reduction, bound.

The successful simulation of the data in Fig. 3 allows an important conclusion that H_2 is evolved before either N_2H_4 or NH_3 is detected (see Thorneley & Lowe, 1984*a*). Thus H_2 is the first reduction product to be released by nitrogenase in the catalytic cycle of N_2 fixation. The simulation also requires that a stoichiometric release of H_2 occurs when N_2 binds to species E_3H_3 and E_4H_4. The significance of this is discussed in the following paper (Thorneley & Lowe, 1984*a*) together with the N_2-binding reaction and the pre-steady-state kinetics of N_2H_4 and NH_3 formation.

A feature of many previous mechanistic studies with nitrogenase is that they either have been concerned with one or more partial reactions in the catalytic cycle or have presented steady-state kinetic data with a necessarily limited analysis and conclusion. The scheme outlined above and developed in the following papers (Thorneley & Lowe, 1984*a*,*b*; Lowe & Thorneley, 1984) is the first unifying theory for nitrogenase action that is capable of explaining all published kinetic data. Although, as stated in the introduction, we have not been able to define the detailed chemistry occurring at the active site(s), we have defined the conditions and times that should be optimal for the detection of the postulated intermediates.

We thank Professor J. R. Postgate for comments on the manuscript, Mr. K. Baker and Miss L. Sones for growing *K. pneumoniae* cells, Mrs. G. Ashby and Mr. K. Fisher for technical assistance, and Dr. R. C. Bray for use of the rapid-quench apparatus.

References

Clarke, L. J. & Axley, H. J. (1955) *Anal. Chem.* **27**, 2000–2005

Burgess, B. K., Wherland, S., Newton, W. E. & Stiefel, E. I. (1981) *Biochemistry* **20**, 5140–5146

Cornish-Bowden, A. (1979) *Fundamentals of Enzyme Kinetics*, pp. 177–199, Butterworths, London

Dilworth, M. J. & Thorneley, R. N. F. (1981) *Biochem. J.* **193**, 971–983

Eady, R. R., Smith, B. E., Cook, K. A. & Postgate, J. R. (1972) *Biochem. J.* **128**, 655–675

Eady, R. R., Lowe, D. J. & Thorneley, R. N. F. (1978) *FEBS Lett.* **95**, 211–213

Guth, J. H. & Burris, R. H. (1983) *Biochemistry* **22**, 5111–5122
Gutteridge, S., Tanner, S. J. & Bray, R. C. (1978) *Biochem. J.* **175**, 869–878
Hageman, R. V. & Burris, R. H. (1978) *Proc. Natl. Acad. Sci. U.S.A.* **75**, 2699–2702
Hageman, R. V. & Burris, R. H. (1980) *Biochim. Biophys. Acta* **591**, 63–75
Hageman, R. V., Orme-Johnson, W. H. & Burris, R. H. (1980) *Biochemistry* **19**, 2333–2342
Lowe, D. J. & Thorneley, R. N. F. (1984) *Biochem. J.* **224**, 895–901
Lowe, D. J., Thorneley, R. N. F. & Postgate, J. R. (1984) in *Advances in Nitrogen Fixation Research* (Veeger, C. & Newton, W. E., eds.), pp. 133–138, Nijhoff-Junk, The Hague, Boston and Lancaster
Miller, R. W., Robson, R. L., Yates, M. G. & Eady, R. R. (1980) *Can. J. Biochem.* **58**, 542–546
Rivera-Ortiz, J. M. & Burris, R. H. (1975) *J. Bacteriol.* **123**, 537–545
Silverstein, R. & Bulen, W. A. (1970) *Biochemistry* **9**, 3809–3815
Smith, B. E., Thorneley, R. N. F., Yates, M. G., Eady, R. R. & Postgate, J. R. (1976) *Proc. Int. Symp. Nitrogen Fixation 1st* **1**, 150–176
Thorneley, R. N. F. (1975) *Biochem. J.* **145**, 391–396
Thorneley, R. N. F. & Lowe, D. J. (1983) *Biochem. J.* **215**, 393–403
Thorneley, R. N. F. & Lowe, D. J. (1984*a*) *Biochem. J.* **224**, 887–894
Thorneley, R. N. F. & Lowe, D. J. (1984*b*) *Biochem. J.* **224**, 903–909
Thorneley, R. N. F., Eady, R. R. & Lowe, D. J. (1978) *Nature (London)* **272**, 557–558
Watt, D. G., Bulen, W. A., Burns, A. & Hadfield, K. L. (1975) *Biochemistry* **14**, 4266–4272